Proceedings 10th NUMGE 2023
10th European Conference on Numerical Methods in Geotechnical Engineering
Zdravkovic L, Kontoe S, Taborda DMG, Tsiampousi A (eds)

https://doi.org/10.53243/NUMGE2023-87

Evaluation of three advanced constitutive models for cyclic loading of sands

D. Konstantinidis[1], C.M. Martin[1], H.J. Burd[1]

[1]*Department of Engineering Science, University of Oxford, Parks Road, Oxford OX1 3PJ, UK*

ABSTRACT: The present work examines the advantages and disadvantages of two widely known constitutive modelling approaches for cyclic loading simulations: i) multi-surface plasticity and ii) bounding surface plasticity. Two multi-surface models and one bounding surface model are implemented and calibrated and their performance at a single element level is examined. Emphasis is placed on the performance of two multi-surface models, namely a series model for cohesionless soils employing nested kinematic hardening yield surfaces, and a parallel Iwan model capable of predicting a Masing-type nonlinear hysteretic response without the need for translating surfaces. The latter, 'PIMSS' (Parallel Iwan Multi-Surface Sand), is a new effective stress model for sands and hence its formulation is briefly described. The predictive capability and ease of calibration of the two multi-surface models are discussed. These models are then compared with a commonly used version of the bounding surface model SANISAND. The model predictions are assessed for drained and undrained monotonic and cyclic undrained triaxial tests focusing on key points such as the phase transformation behaviour of denser sands, stress attractor at liquefaction state and stiffness degradation during undrained cyclic loading.

Keywords: Constitutive models; Monotonic and cyclic loading; Sands; Bounding surface plasticity; Multi-surface plasticity

1 INTRODUCTION

Cyclic loading is important for the design of offshore wind turbine (OWT) foundations. The numerical simulation of OWT foundations demands the utilisation of appropriate constitutive models. During the last decades, many sophisticated constitutive models have been proposed and used with success for simulating the monotonic loading of sands. However, the capabilities of these models are more limited when it comes to simulating the behaviour of sands under cyclic loading (Wichtmann et al. 2019). Also, these models typically require extensive calibration procedures and they are often incapable of reproducing accurately all loading conditions with a single set of parameters. The purpose of this paper is to evaluate the performance and indicate the strengths and weaknesses of three constitutive models: the Prevost sand model in its original version (Prevost 1985), the 2008 version of the SANISAND model (Taiebat and Dafalias 2008), denoted here as 'SANISAND08', and the initial version of a new effective stress model, 'PIMSS', employing a parallel Iwan approach.

This study utilizes the experimental data from laboratory tests performed on Karlsruhe fine sand (Wichtmann and Triantafyllidis 2016a, 2016b). Selected laboratory tests have been simulated with the three constitutive models and their predictive capability is assessed. This paper will only focus on medium dense sand samples (which is a density condition that is often encountered in offshore conditions). Sands of this density are expected to exhibit salient behavioural features under the examined loading conditions and therefore these laboratory data can be used as a good reference for benchmarking the three constitutive models. Observable aspects anticipated in drained conditions are the transition from contractive to dilative volumetric response and a peak shear strength which reduces to a residual value at high strains. In undrained loading, tendency for volume changes is expressed through the development of excess pore water pressures, inducing stiffness degradation during cyclic loading.

The three models have been implemented in MATLAB. First, the formulation and the calibration of the models are briefly discussed and subsequently the results of single element simulations incorporating these models are compared with the respective laboratory tests.

2 BRIEF DESCIPTION OF MODELS

For brevity the constitutive equations of the Prevost and the SANISAND08 models are not included here, but can be found in the respective original papers cited previously. The basic equations of PIMSS are shown, but its formulation will be described in more detail in future publications. All models are implemented in the multiaxial three-dimensional stress space adopting a simple forward Euler stress integration scheme.

2.1 Series multi-surface plasticity model

The first model is the original version of the Prevost multi-surface plasticity formulation proposed for cohesionless soils (Prevost 1985). The multi-surface plasticity concept was first conceived by Iwan (1967) and Mroz (1967). Iwan proposed two different one-dimensional models, termed as 'parallel-series' and 'series-parallel' respectively and eventually extended the latter to three dimensions. The idea of the three-dimensional formulation of the Iwan series-parallel continuum model is similar to the one proposed by Mroz (1967) and subsequently by Prevost (1985). In the present paper the term 'series' is used as short for 'series-parallel' and specifically its three-dimensional continuum extension, whereas 'parallel' is used to refer to 'parallel-series' respectively.

The Prevost model incorporates a family of nested homothetical surfaces yield surfaces, which are conical in principal stress space. These surfaces are subjected to kinematic hardening via a purely deviatoric hardening rule. This is the way that this approach achieves the discretisation of the plastic moduli inducing hardening behaviour. The deviatoric plastic flow of the model is associated, but the volumetric plastic flow component is non-associated. The only difference between the present implementation and the original formulation (Prevost 1985) is that the volumetric flow component is scaled by a scalar parameter ψ, as documented by Cerfontaine (2014). This can be better understood from Equation (5) ignoring the superscript i as the plastic potential in the Prevost model is unique for all surfaces. With the scalar ψ the magnitude of dilatancy becomes adjustable and a better fit can be achieved for monotonic tests.

2.2 Parallel multi-surface plasticity model

PIMSS is also a multi-surface model. However, in contrast to the Prevost model, PIMSS does not employ any kinematic hardening rules and its surfaces remain stationary. Consistent with Iwan's original one-dimensional concept, the parallel Iwan approach has been adopted as the basis for the development of continuum plasticity soil models. An example for clays is the model by Whyte et al. (2020) and for sands by Dawson (2013).

When this approach is employed to develop a constitutive model, a number of individual micro-models are arranged in parallel and therefore are subjected to the same strain history (Whyte et al. 2020). The resulting macro-stress tensor (σ) is calculated as the weighted sum of the individual micro-stress tensors (σ_{micro}) as:

$$\sigma = \sum_{i=1}^{n} w_i \cdot \sigma_{micro} \tag{1}$$

where n is the total number of micro-models and w_i is the weight corresponding to each micro-model. The sum of the weights must be equal to unity ($\sum_{i=1}^{n} w_i = 1$). This approach can produce a Masing type non-linear response, without the need for translating surfaces and hence kinematic hardening and mapping rules. Another advantage of this concept is that each micro-model is numerically implemented as a single-surface plasticity model, which eases the implementation of the overall macro-model.

The main motivations for the development of PIMSS were two. First, the parallel Iwan approach has been used with success for the simulation of monopile foundations in clay, subjected to monotonic and cyclic lateral loading (Whyte et al. 2020). Second, prompted by the predictive capability of the Prevost model (Cerfontaine 2014), it was considered worth investigating how a parallel version of the model with no kinematic hardening would perform.

Hence, PIMSS is a parallel arrangement of several stationary micro-models incorporating the same yield surface, plastic potential, and elasticity as the Prevost model. Specifically, the yield surface equation of the ith micro-model is of the form,

$$f^i = \boldsymbol{s}^i : \boldsymbol{s}^i - \frac{2}{3}\left(p^i \cdot M^i\right)^2 = 0 \tag{2}$$

where $\boldsymbol{s}^i$and p^i are the deviatoric stress tensor and the mean effective stress respectively and M^i is a material parameter denoting the aperture of the cone of each micro-model. The plastic potential $\boldsymbol{P}^i$ of each micro-model is decomposed into its deviatoric component, which is associative, and its volumetric component, which is non associative as:

$$\boldsymbol{P}^i = (\boldsymbol{P}^i)' + (P^i)'' \cdot \boldsymbol{\delta} \tag{3}$$

$$\left(\boldsymbol{P}^i\right)' = \left(\boldsymbol{Q}^i\right)' = \frac{2 \cdot \boldsymbol{s}^i}{\left\| \frac{\partial f^i}{\partial \boldsymbol{\sigma}^i} \right\|} \tag{4}$$

$$(P^i)'' = \frac{\psi^i}{3} \cdot \frac{(\eta^i)^2 - (\bar{\eta}^i)^2}{(\eta^i)^2 + (\bar{\eta}^i)^2} \text{ and } \eta^i = \frac{(3/2 \cdot \boldsymbol{s}^i : \boldsymbol{s}^i)^{1/2}}{p^i} \tag{5}$$

where $(\boldsymbol{P}^i)'$ is the deviatoric component of the plastic potential and $(P^i)''$ is its volumetric component, $(\boldsymbol{Q}^i)'$ is the deviatoric part of the second-order tensor $\boldsymbol{Q}^i$ that defines the unit outer normal to the yield surface, ψ^i is a material parameter scaling the volumetric component of the plastic potential and $\bar{\eta}^i$ is a material parameter, which denotes the stress ratio at phase transformation. Regarding the elastic part of each micro-model, the dependency of stiffness on the mean effective stress is considered as follows:

$$G^i(p^i) = {G_0}^i \cdot \left(\frac{p^i}{p_{ref}}\right)^n \tag{6}$$

where G^i is the shear stiffness, p_{ref} is the reference pressure, ${G_0}^i$ is the small-strain shear modulus and n is

usually taken as 0.5 for most cohesionless soils (Prevost 1985). K^i is obtained from $K = 2G(1+\nu)/3(1-2\nu)$ by introducing a constant Poisson's ratio ν.

2.3 Bounding surface plasticity model

The SANISAND family of models is formulated in the framework of critical state soil mechanics and bounding surface plasticity. Many versions of SANISAND have been proposed capturing different aspects of sand behaviour with two recent versions performing remarkably well under cyclic loading (Liu et al. 2020, Yang et al. 2022). The 2008 formulation was chosen for the present study, because there are no simulations involving cyclic loading adopting this version available in literature and it is of interest to investigate how it performs.

3 PARAMETER CALIBRATION

The parameters adopted for the Prevost model for Karlsruhe fine sand with a relative density D_{r0} in the range 57 to 68% are summarized in Table 1. The values of the parameters were determined following the procedure described by Prevost (1985). The surface specific parameters M, H' and α were estimated using drained triaxial tests. Initially, the experimental stress-strain curve of a triaxial compression test ($D_{r0} = 63\%$, cell pressure of 100kPa) is represented by linear segments of constant plastic moduli H'. The number of segments corresponds to the number of surfaces selected for the model. Having calculated H' from this approximation, the upper and the lower bounds of each of the surfaces in terms of η (where $\eta = {}^{q}/_{p}$) are needed to estimate M and α. The upper bounds, η_c, are assumed to be at the transition points between two segments of the triaxial compression curve. The lower bounds, η_e, can be found by repeating this procedure using a drained extension test at the same cell pressure. The database used is lacking this type of experimental data, so a fictitious extension curve was used instead, assuming that $\eta_e = 0.60 \cdot \eta_c$. Having found the upper and lower bounds of each surface in terms of η, the calculation of M and α is straightforward. In the absence of data from bender element tests or local strain instrumentation, the elastic parameter G_0 was estimated as the secant shear stiffness, assuming a very small purely elastic initial part on the ε_1-q curve. In theory to accurately capture the volumetric response of a drained triaxial test the parameter $\bar{\eta}$ should be taken as the stress ratio where dilative response starts taking place. In practice, the value of $\bar{\eta}$ needs to be adjusted by trial-and-error procedure, so that good fit is achieved for both drained and undrained tests, as well as monotonic and cyclic loading. The same applies to ψ.

Table 2 contains the parameters adopted for PIMSS for the same sand. PIMSS was calibrated by fitting the backbone stress-strain curve of a drained triaxial compression test. The test used was the same as for the Prevost model. Two main approaches can be used to calibrate a parallel model when fitting a backbone curve, either by distributing the strength parameters of its components but assigning the same weighting to all of them or by additionally distributing the component weightings (Dawson 2013). For the present study the first approach was used. Even though this approach is similar to the calibration process adopted for the surface-specific parameters of the Prevost model, it is slightly more elaborate as the overall model behaviour is the averaged behaviour of several components. Regarding the plastic potential parameters $\bar{\eta}$ and ψ, the micro-models have been classified into two groups. Micro-models 1-7 are assigned with values of parameters that induce a purely contractive behaviour, whereas micro-models 8-15 initially a produce smaller contractive response but rather pronounced dilation subsequently. The combination of these two groups of micro-models gives the desired monotonic overall response. As can be seen in Table 2, two values are given for these parameters, as they had to be adjusted to achieve the desired cyclic fit. The values used for the cyclic simulations are the ones in parentheses.

Table 1. Material parameters of Prevost model for Karlsruhe fine sand used for the single element simulations.

Surface	**1**	**2**	**3**	**4**	**5**	**6**	**7**	**8**	**9**	**10**	**11**	**12**	**13**	**14**	**15**
$\boldsymbol{M}$ **[-]**	0.074	0.178	0.546	0.744	0.838	0.906	1.018	1.114	1.165	1.201	1.222	1.236	1.244	1.249	1.25
$\boldsymbol{H'}$ **[-]**	70	22	15	8	3	2	0.9	0.6	0.3	0.25	0.2	0.1	0.05	0.01	0.001
$\boldsymbol{\alpha}$ **[-]**	0.019	0.045	0.137	0.186	0.209	0.227	0.255	0.278	0.291	0.3	0.305	0.309	0.311	0.312	0.312
Global	$\boldsymbol{G_0}$ **[MPa]**		$\boldsymbol{K_0}$ **[MPa]**		$\bar{\boldsymbol{\eta}}$ **[-]**		$\boldsymbol{\psi}$ **[-]**								
	30		20		1.19		0.8								

Table 2. Material parameters of PIMSS model for Karlsruhe fine sand used for the single element simulations.

Surface	**1**	**2**	**3**	**4**	**5**	**6**	**7**	**8**	**9**	**10**	**11**	**12**	**13**	**14**	**15**
$\boldsymbol{w}$ **[-]**	0.062	0.067	0.067	0.067	0.067	0.067	0.067	0.067	0.067	0.067	0.067	0.067	0.067	0.067	0.067
$\boldsymbol{M}$ **[-]**	0.124	0.211	0.4	0.64	0.838	1.0	1.2	1.4	1.5	1.6	1.8	2.0	2.05	2.15	2.3
$\boldsymbol{G}$ **[kPa]**	37	34	33	32	30	28	25	20	19	17	15	13	10	7	5
Micro-models 1-7	$\bar{\boldsymbol{\eta}}$ **[-]**			$\boldsymbol{\psi}$ **[-]**			**Micro-models 8-15**	$\bar{\boldsymbol{\eta}}$ **[-]**			$\boldsymbol{\psi}$ **[-]**				
	$2M^i$ ($2.5M^i$)			1.7 (0.9)				$0.5M^i$ ($1.3M^i$)			1.1 (0.9)				

Table 3. Material parameters of SANISAND (2008) model for Karlsruhe fine sand used for the single element simulations.

e_0 [-]	λ [-]	ξ [-]	α_c^c [-]	c [-]	m [-]	G_0 [-]	ν [-]	h_0 [-]	c_h [-]	n_b [-]	A_0 [-]	n_d [-]	ρ_r [kPa]	ρ_c [-]	ϑ [-]	X [-]
1.103	0.122	0.205	1.29	0.7	0.05	150 (100)	0.05	10.5	0.75 (1.0)	1.2	0.9	2.0	-	-	-	-

Table 3 summarises the parameters adopted for the SANISAND08 model. The first thirteen parameters shown in the table are taken from previous work where a SANISAND version was used (Wichtmann et al. 2019). The last four parameters are not shown because the component of the model requiring them was deactivated in all simulations. The type of loading associated with this constitutive ingredient is not in the scope of the present study. Parameters G_0 and c_h had to be adjusted for the cyclic simulations, as the values used for the monotonic tests resulted in unrealistic behaviour. The values used for the cyclic simulations are contained in the parentheses.

As SANISAND08 is the only critical state dependent formulation out of the three, its parameters need to be calibrated only once irrespective of the initial density and stress level. The other two models are pressure dependent and therefore their parameters can cope with different initial pressures, but a new set of parameters would be needed for different densities. It can also be concluded that the Prevost model was the only one out of the three to be given a single set of parameters for both monotonic and cyclic loading conditions.

4 SINGLE ELEMENT SIMULATIONS

4.1 Monotonic triaxial tests

Figure 1 presents simulations of monotonic drained triaxial compression tests of medium dense sand samples ($57\% \leq D_{r0} \leq 68\%$) with different initial stresses (cell pressures of 50, 100, 200 and 400kPa). All three constitutive models could accurately represent the dependence of the stress-strain response on the initial stress level. The Prevost and PIMSS models give stress-strain curves almost identical to each other. These two multi-surface models do not accomodate softening behaviour in their current formulations. Therefore, both models were calibrated to reach the peak strengths exhibited in the laboratory with no subsequent reduction of their strength to a critical value at large strains. This lead to an overestimation of the shear strength predicted at large strain levels. However, this limitation does not apply to typical offshore applications as soil strains in typical design calculations are not expected to exceed about 10%. In contrast, SANISAND08 is able to reproduce softening at higher strains attaining a critical value of strength by the end of the test, giving a very good overall match with the experimental data. More differences are observed between the simulations and the experiments with respect to the volumetric response of the sand samples. Specifically, both Prevost and PIMSS models overpredicted the compression experienced by the sand with the latter model deviating more from the data. Both PIMSS and Prevost predicted dilation, which continues unceasingly at a constant rate, which is unrealistic, as a terminal density is expected to be attained at high strains. SANISAND08 was able to simulate this behaviour, but was not able to clearly show the dependence of the volumetric behaviour on the stress level for samples with cell pressures of 50 and 100kPa.

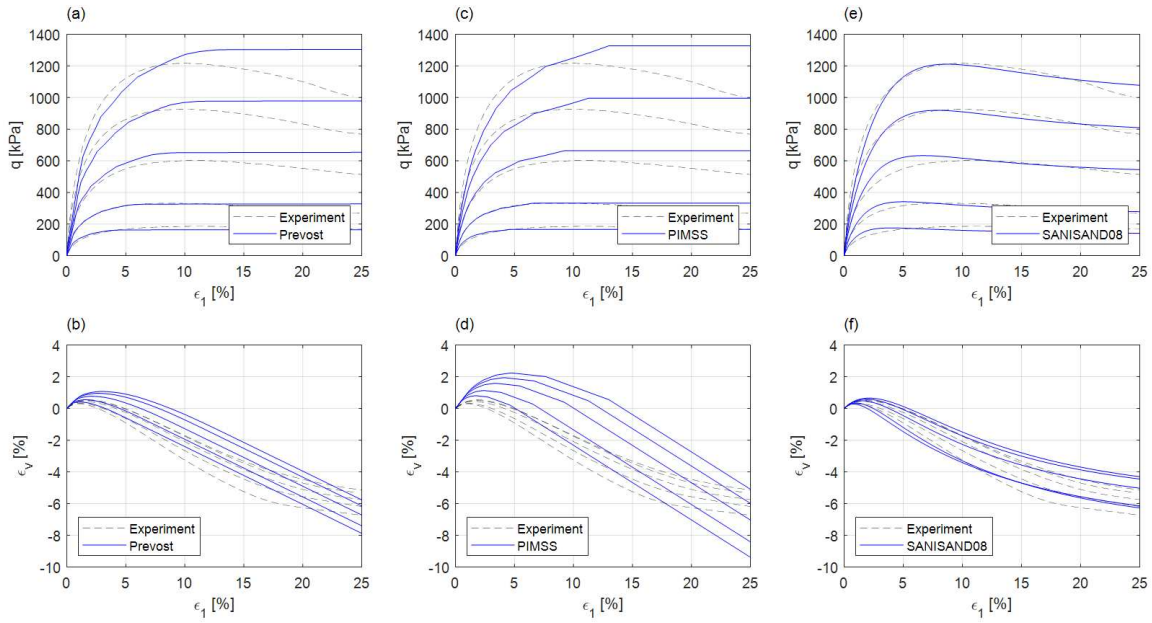

Figure 1. Simulations of drained monotonic triaxial tests on medium dense samples ($57\% \leq D_{r0} \leq 68\%$) with different initial stresses (cell pressures of 50, 100, 200 and 400kPa): a,b) Prevost, c,d) PIMSS, e,f) SANISAND08.

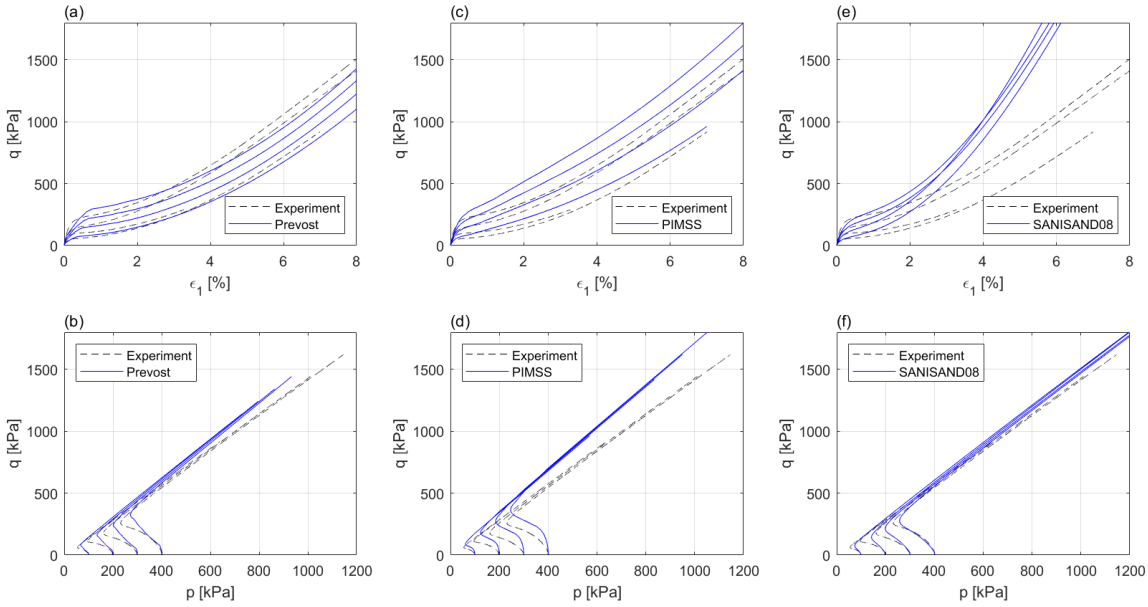

Figure 2. Simulations of undrained monotonic triaxial tests on medium dense samples ($60\% \leq D_{r0} \leq 64\%$) with different initial stresses (cell pressures of 100, 200, 300 and 400kPa): a,b) Prevost, c,d) PIMSS, e,f) SANISAND08.

Figure 2 presents simulations of undrained monotonic triaxial tests on medium dense sand samples ($60\% \leq D_{r0} \leq 64\%$) with different initial stresses (cell pressures of 100, 200, 300 and 400kPa). From the upper row it can be seen that both PIMSS and the Prevost model gave a fairly accurate stress-strain response. However, the curves reproduced with SANISAND08 deviate from reality with the latter significantly overpredicting the tendency of the sand to dilate. The lower row of Figure 2 shows the respective effective stress paths in the p-q space. All three models managed to reproduce at least qualitatively all the salient aspects of sand behaviour associated with the development of pore water pressures and its effect on the effective stresses. All of them were able to show a phase transformation from positive values of pore pressure initially and hence reduction of the effective stresses, to negative pore pressures and the respective increase of the effective stresses as the loading proceeds. The Prevost and PIMSS models seem to slightly overpredict the slope of the failure line, whereas SANISAND08 captures that very accurately. Similarly to the stress-strain curves, SANISAND08 siginificantly overpredicts the tendecy of the sand to dilate by predicting large negative values of pore pressures. Even though only a zoomed version of the results is shown (Figure 2(f)) it is worth noting that the simulation with SANISAND08 predicts a deviatoric stress path up to almost 2400kPa.

4.2 Cyclic triaxial tests

Figure 3 shows simulations of an undrained cyclic triaxial test on a medium dense sand sample ($D_{r0} = 66\%$) after isotropic consolidation. Large strain ampitudes are applied to the sample. The upper row of Figure 3 shows the stress-strain response predicted by the three models. It is seen that only the Prevost and PIMSS models can predict adequately the softening that occurs in the sand sample, with the Prevost model being more accurate. SANISAND08 predicts almost no degradation. The lower row of Figure 3 indicates that only the stress path simulated by the Prevost model manages to finally arrive at the origin p=q=0, correctly predicting that the sand sample liquefies. However, the numerical simulation predicts that liquefaction will take place after a smaller number of cycles than in the laboratory. The stress paths reproduced by PIMSS and SANISAND08 both exhibit shearing locking patterns approximately 40-50kPa away from the origin, not being able to predict liquefaction. The inability of PIMSS to predict this behaviour, as opposed to the Prevost model, implies that the absence of kinematic hardening from the first should be compensated with additional constitutive mechanisms that will aid simulations of this type. Similarly for SANISAND08, this inability probably stems from the absence of constitutive ingredients acounting for cyclic mobility effects.

5 CONCLUSIONS

Three advanced constitutive models for sand were calibrated, and their predictive capability was assessed. All three could reproduce basic aspects of sand experimental behaviour well, each of them with specific limitations related to their formulations. It was shown for all the models, that it is not possible to accurately simulate all types of loading conditions with a single set of parameters, without compromising their capability to reproduce important behavioural features expected from sands of specific density and initial stress level.

Also, a practical multi-surface effective stress model, PIMSS, employing a parallel arrangement of stationary micro-models, was proposed for the simulation of the monotonic and cyclic behaviour of sand. Results from single elements simulations with PIMSS are promising. This formulation is robust in terms of numerical implementation allowing for future modifications and enhancements that will further improve its predictive capability.

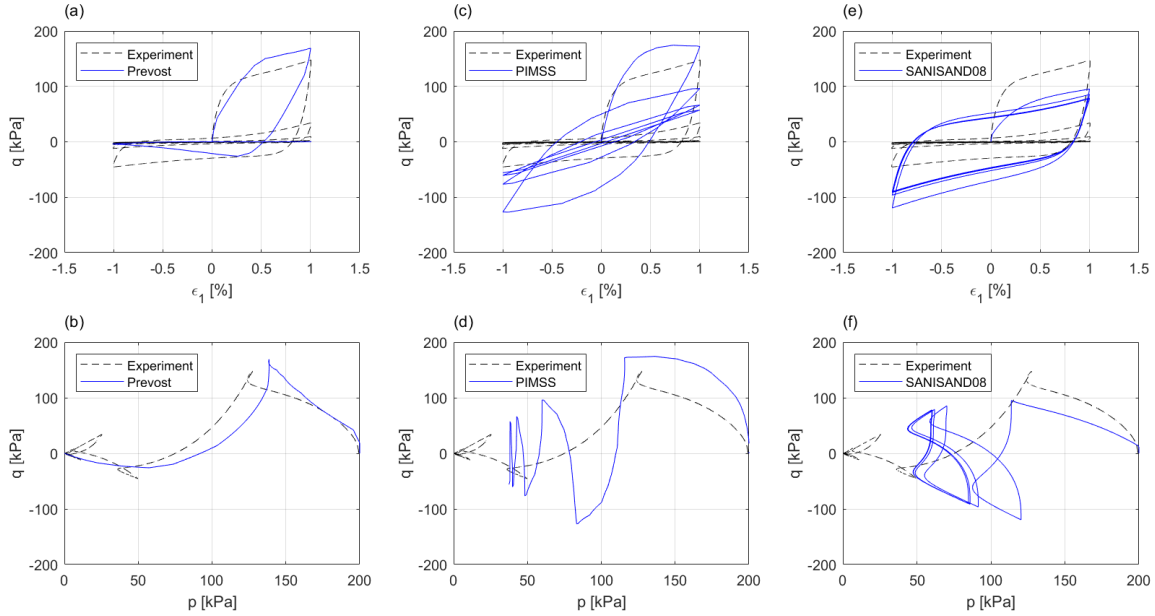

Figure 3. Simulations of an undrained cyclic triaxial test on medium dense sample ($D_{r0} = 66\%$) with isotropic consolidation (cell pressure of 200kPa) large-amplitude strain cycles ($\varepsilon_1^{ampl.} = 1 \cdot 10^{-2}$): a,b) Prevost, c,d) PIMSS, e,f) SANISAND08.

6 ACKNOWLEDGEMENTS

The first author gratefully acknowledges the financial support of Fugro GB Marine Limited.

7 REFERENCES

Cerfontaine, B. 2014. The cyclic behaviour of sand, from the Prevost model to offshore geotechnics. Doctoral Dissertation, Université de Liège.

Dawson, E.M. 2013. A parallel Iwan model for 3D cyclic loading of frictional materials. *In* Proceedings of the 3rd International FLAC/DEM Symposium. Itasca International, Hangzhou, China.

Iwan, W.D. 1967. On a class of models for the yielding behavior of continuous and composite systems. Journal of Applied Mechanics, **34**(3): 612–617.

Liu, H., Diambra, A., Abell, J.A., and Pisanò, F. 2020. Memory-Enhanced Plasticity Modeling of Sand Behavior under Undrained Cyclic Loading. Journal of Geotechnical and Geoenvironmental Engineering, **146**(11). American Society of Civil Engineers (ASCE).

Mroz, Z. 1967. On the description of anisotropic workhardening. J. Mech. Phys. Solids, **15**: 163–175. Pergamon Press Ltd.

Prevost, J.H. 1985. A simple plasticity theory for frictional cohesionless soils. International Journal of Soil Dynamics and Earthquake Engineering, **4**(1): 9–17.

Taiebat, M., and Dafalias, Y.F. 2008. SANISAND: Simple anisotropic sand plasticity model. International Journal for Numerical and Analytical Methods in Geomechanics, **32**(8): 915–948.

Whyte, S.A., Burd, H.J., Martin, C.M., and Rattley, M.J. 2020. Formulation and implementation of a practical multi-surface soil plasticity model. Computers and Geotechnics, **117**. Elsevier Ltd.

Wichtmann, T., Fuentes, W., and Triantafyllidis, T. 2019. Inspection of three sophisticated constitutive models based on monotonic and cyclic tests on fine sand: Hypoplasticity vs. Sanisand vs. ISA. Soil Dynamics and Earthquake Engineering, **124**: 172–183. Elsevier Ltd.

Wichtmann, T., and Triantafyllidis, T. 2016a. An experimental database for the development, calibration and verification of constitutive models for sand with focus to cyclic loading: part I—tests with monotonic loading and stress cycles. Acta Geotechnica, **11**(4): 739–761. Springer Verlag.

Wichtmann, T., and Triantafyllidis, T. 2016b. An experimental database for the development, calibration and verification of constitutive models for sand with focus to cyclic loading: part II—tests with strain cycles and combined loading. Acta Geotechnica, **11**(4): 763–774. Springer Verlag.

Yang, M., Taiebat, M., and Dafalias, Y.F. 2022. SANISAND-MSf: A sand plasticity model with memory surface and semifluidised state. Geotechnique, **72**(3): 227–246. ICE Publishing.